#13157

World Renewable Energy Congress VI (WREC2000)

Editor: A.A.M. Sayigh

EVALUATION OF VERTICAL SOLAR-AIR COLLECTORS FOR NATURAL VENTILATION USING INTEGRAL AND CFD MODELS

A. Moret Rodrigues[1]; A. Canha da Piedade[1]; H. Awbi[2]

[1]*Instituto Superior Técnico/ICIST - Av. Rovisco Pais, 1049-001 Lisboa, PORTUGAL*

[2]*Department of Construction Management & Engineering, The University of Reading, UK*

ABSTRACT

Vertical solar-air collectors that are used for providing natural ventilation can be a viable solution in buildings where higher ventilation rate requirements for better indoor air quality cannot be met by traditional natural ventilation methods. Indoor air quality problems have been experienced in Portuguese school buildings where a study revealed that the CO_2 concentrations in classrooms in winter were higher than the recommended health limits. To improve the environment in these classrooms, solar-induced ventilation has been suggested. In the design of these solar ventilators, simple models can only predict the main features of the flow but they can be useful tools in the first stages of the design process. However, CFD models can produce microscopic information about the state of all flow parameters and thus are recommended when a high degree of accuracy is needed. In this paper, a simplified model based on the integral equations of motion and heat transfer is developed for a vertical solar-air collector and applied to different boundary conditions. The results are compared and discussed with those computed from a CFD code specially designed for room ventilation.

KEYWORDS: solar-air collector; Trombe wall; natural ventilation; buoyant flow.

INTRODUCTION

The vertical channel which is open at both ends and subjected to different wall thermal conditions, has been an important topic of natural heat convection research due to its wide engineering applications. The interest in such a device is the natural buoyant flow that can be produced by simply heating or cooling a four-sided vertical wall system in a stagnant surrounding fluid at a different thermal state. As the gap fluid temperature is different from that prevailing outdoors, an unbalanced buoyancy force arises which sets the channel fluid in motion. The resulting flow configuration is dependent upon the wall conditions.

One of the applications recognised as being of practical interest is the use of the heated channel principle – known as a "Trombe wall" - for increasing room ventilation rates in winter or summer using solar energy. The individual system consists basically of two main vertical parallel plates – one transparent and the other heat absorbent - forming a flat channel able to be integrated with the building façade, preferably on those exposed to the sun. With the solar radiation acting as the heating source, the system works as an air collector, with a link between the indoor and outdoor environments through two openings placed at the channel extremities. This system has been used to ventilate classrooms in a prototype Portuguese school building (Moret Rodrigues *et al.*, 1996) where indoor CO_2 measurements in winter have revealed concentrations higher than the recommended health limits.

Flow rates provided by this type of systems can be predicted by simple or more complex methods, the preference for one or another depends on the required accuracy of the results. CFD models are an example

of the latter ones. For a discretized domain, they locally solve the complete set of the conservation equations of momentum, mass and energy, using numerical methods well documented in the literature. This fact can render this class of models costly in terms of the necessary computing resources of which the machine calculation time and memory capacity are typical examples. Therefore, they happen to be not suitable for very large or multi-zone domains involving complex heat transfer processes. In these cases, simple methods, currently used in the so-called network (zonal) models, appear to be a reasonable option, mainly when only average values are required. This advantage can justify the efforts in the development or improvement of such methods, referred to here as simplified, which may become eventually powerful tools for use in engineering design.

This paper focuses on an integral analysis of the natural buoyant channel system, taken as simple as possible, in order to study the relevant parameters which govern the flow. In addition, results from CFD computations are presented and compared with those from the integral model. Given that heat fluxes (rather than temperatures) are the natural channel wall conditions due to the action of solar radiation, only the channel flow induced by uniform heat fluxes will be analysed here, although using different heating power for each wall. In real working conditions and due to the magnitude of the heat input and channel geometry, the flow within the channel is expected to be in the turbulent regime most of the time. For this reason, the present paper will only deal with turbulent flow, in the assumption that it starts just after the entrance to the channel.

INTEGRAL MODEL

The model is based on the differential form of the generalised Bernoulli equation and the energy equation, respectively given by

$$d\left(\frac{\alpha u_s^2}{2}\right)+g\,dx+\frac{dp_s}{\rho_s}=-\frac{|dW_f|}{\dot m} \tag{1}$$

$$\dot m c_p dT_s=\chi q_w dx \tag{2}$$

where H is the height and $\chi=2(l+e)$ is the channel perimeter.

The heat flux on the solid boundaries is assumed uniform (Neumann conditions), as shown in Fig. 1, i.e., $q_w=\left[l\left(q_{w_y}^-+q_{w_y}^+\right)+e\left(q_{w_z}^-+q_{w_z}^+\right)\right]/\chi$. In these equations, the velocity, density, temperature and pressure are average quantities defined as:

$$u_s=\frac{1}{S}\int_S u\,dS \qquad \rho_s=\frac{1}{u_s S}\int_S \rho u\,dS \qquad T_s=\frac{1}{\dot m}\int_S \rho\, u T\,dS \qquad p_s=\frac{1}{u_s S}\int_S p\,u\,dS$$

where u is the stream-wise velocity and $\dot m=\int_S \rho\,u\,dS=\rho_s u_s S$ is the constant mass flux. The term on the right side of (1) represents the loss of energy per unit fluid mass, due to friction (on channel surfaces and internally), and can be written in the form:

$$-\frac{|dW_f|}{\dot m}=-\Psi\frac{u_s^2}{2}\frac{dx}{D_h}$$

where $D_h\equiv 4\times\text{area}/\text{perimeter}=2\times(l\times e)/(l+e)$ is the hydraulic diameter of the channel and Ψ is a parameter which depends on the expression used for the viscous losses. If the concept of shear stress coefficient is used, the proper relationship is $\Psi=4c_f$. The velocity across the section is also presented in equation (1) by the kinetic-energy correction factor, defined as:

$$\alpha=\int_S \rho v^2 u\,dS/(u_s^2\dot m)$$

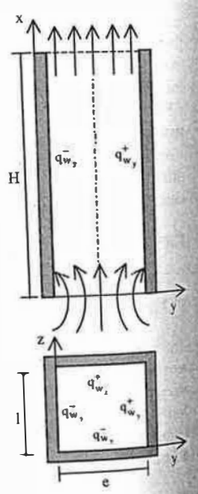

Fig.1– Collector model

where v is the flow velocity. With respect to the energy equation (2), the form presented does not include the viscous dissipation term and the rate of change of pressure as they are of minor importance in building ventilation. The integration of this equation gives:

$$T_{s,x}=T_{s,0}(1+\Lambda x) \tag{3}$$

where, $\Lambda=q_w\chi/(\dot m c_p T_{s,0})$.

The perfect gas law and the assumption of small pressure variations ($\rho T\approx$ constant) gives:

$$\rho_{s,x}/\rho_{s,0}=T_{s,0}/T_{s,x}=1/(1+\Lambda x)$$

In addition, from the condition of constant mass flux $\rho_{s,x}u_{s,x}=\rho_{s,0}u_{s,0}$, the following relation involving the velocities also applies:

$$u_{s,x}/u_{s,0}=1+\Lambda x$$

Finally, concerning the friction coefficient, the following generic form is considered

$$c_{f,x}=a\,Re_x^n=a(\rho_s u_s x/\mu)^n=a(\rho_{s,0}u_{s,0}/\mu)^n x^n=a\,Re_{Dh}^n(x/D_h)^n \tag{4}$$

in which $Re_{Dh}=\rho_s u_s D_h/\mu$ is a Reynolds number based on the hydraulic diameter, μ is the dynamic viscosity and a and n are parameters.

Integrating equation (1) using the above relationships with a constant value for α (normally, α is close to unity in turbulent flow), gives:

$$p_{s,x}=p_{s,0}-\frac{2a\rho_{s,0}u_{s,0}^2 Re_x^n x}{D_h}\left(\frac{1}{n+1}+\frac{\Lambda x}{n+2}\right)-g\rho_{s,0}\frac{\ln(1+\Lambda x)}{\Lambda}-\alpha\rho_{s,0}u_{s,0}^2\Lambda x \tag{5}$$

At the inlet, the flow contraction – Fig. 1 - gives rise to a minor loss, which can be expressed by:

$$p_{0,atm}-p_{s,0}=\frac{\rho_{s,0}}{2}\left(\frac{u_{s,0}}{C_d}\right)^2 \tag{6}$$

where $p_{0,atm}$ is the hydrostatic pressure at the inlet and C_d is the discharge coefficient. At the outlet, the streamlines are approximately parallel (Fig. 1) and the pressure distribution across the outlet jet can be assumed equal to atmospheric pressure, i.e.

$$p_{s,H}=p_{H,atm} \tag{7}$$

therefore,

$$p_{H,atm}=p_{0,atm}-\rho_{s,0}gH \tag{8}$$

Combining the relations (5-8) gives the mass flow rate produced by a system of height H:

$$\dot m=\sqrt{\frac{\left(H-\frac{\ln(1+\Lambda H)}{\Lambda}\right)\rho_{s,0}^2 g}{\frac{2aHRe_H^n}{S^2D_h}\left(\frac{1}{n+1}+\frac{\Lambda H}{n+2}\right)+\frac{1}{2}\left(\frac{1}{C_d S}\right)^2+\frac{\alpha\Lambda H}{S^2}}} \tag{9}$$

It can be seen that for a given geometry and heating conditions, the flow rate as given by equation (9) depends on the values of C_d, a and n. The first depends on the inlet configuration which is responsible for the flow contraction, and usually varies between 0.60 to 1.0. The others depend mainly on the type of flow (external, internal), the flow regime (laminar, turbulent) and the state of flow development. Correlations

combining a and n in the form of equation (4) are available in the literature for different cases and can be used in equation (9).

CFD MODEL

The CFD code used here - VORTEX (Awbi, 1996) - is specially designed for room ventilation. It numerically solves the differential equations that govern the air movement and heat transfer - continuity, momentum and thermal energy - in their elliptic form. The program allows for the turbulent nature of the flow by solving two additional equations for the kinetic energy and energy dissipation rate which are the bases of the so called $\kappa-\varepsilon$ turbulence model. The numerical scheme uses a staggered 3-D Cartesian system where equations are discretized using the Finite Volume Method (FVM) and solved by the well-known SIMPLE algorithm. To enhance the stability of the numerical solution under-relaxation techniques are applied to all the equations. Although the code is capable of solving 3-D flows, in this study only a 2-D solutions were used. This modelling option is more realistic in view of the current channel geometry and spatial wall flux distribution, on the one hand, and the prospect of increased accuracy by using finer grid, on the other.

RESULTS AND DISCUSSION

The CFD and Integral model (INT) were applied to a 2-D channel with height and width of 2.5m and 0.3m, respectively, with a wall flux relation of $q_w^- / q_w^+ = 1/4$. Taking the hotter wall flux q_w^+ as a reference, in the case of the CFD model the calculations were performed for 40, 80, 120, 160 and 200 W per meter of channel height. For the INT model, the mean wall flux has been expressed as $q_w = (q_w^- + q_w^+)/2$ (since this model does not accounts for the wall flux asymmetry), using values for q_w of 25, 50, 75, 100, 125 and 150 W per meter of channel height.

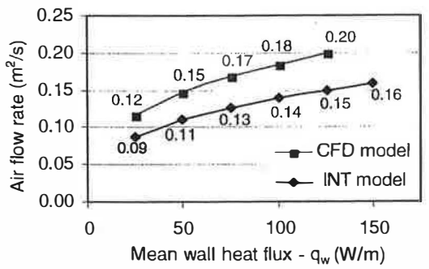

Fig. 2 – Volumetric flow rate

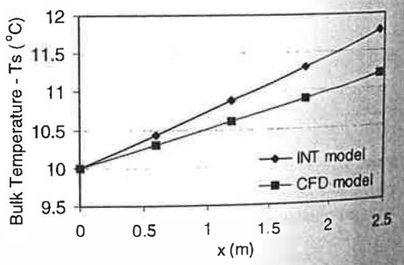

Fig. 3 – Bulk temperature (q_w=50 W/m)

In Fig. 2, the volumetric flow rates produced by the collector system are shown for each model at the channel entrance. As it would be expected, in both models the flow rate increases with the heating power but the rate of change decreases with increasing the wall flux. Although the agreement between the results produced by the two models is not perfect, the discrepancies are within acceptable limits, given the great difference between the two models in terms of complexity of their algorithms.

The bulk temperature of the channel flow, defined by equation (3), is shown in Fig. 3 for the CFD and INT models for the heating case q_w=50 W/m. It can be seen that the two profiles are quite linear. This feature is predicted by equation (3) for the INT model and is well followed by the CFD model, although with a different slope. Nevertheless, the difference in the results from the two models is consistent with the flow rates that each model predicts to satisfy the energy conservation condition. This requires that all the thermal energy transferred to the flow from the channel walls, that is $2q_wH$, must be equal to that at the channel exit. This constraint is the same for both models and as the flow predicted by the INT model is

higher than that from the CFD, then according to equation (2), its bulk temperature should be correspondingly lower so that the condition referred to can be met.

The temperature and stream-wise velocity profiles predicted by the CFD code are plotted for the heating case q_w=50 W/m in Figs. 4 and 5, respectively. The type of profiles observed are consistent with the present heating conditions and channel geometry as has been found in the study by Borgers and Akbari (1984) , although in their case computations were performed for uniform wall temperatures instead of fluxes. In the present case, the profiles show some similarity to those of forced flow, although a clear difference is evident by the skewness in the velocity profile towards the hotter wall by the higher value attained there.

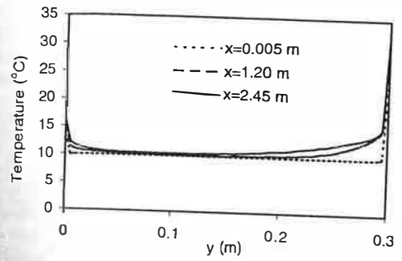

Fig. 4 – Temperature profile (q_w=50 W/m)

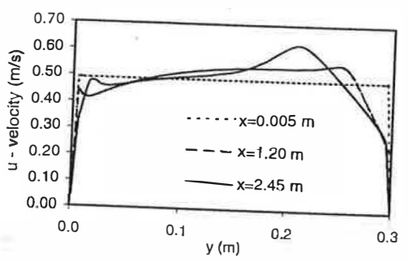

Fig. 5 – u velocity profile (q_w=50 W/m)

The next comparison is with regards to the Nusselt number and is presented in logarithmic scales in Fig. 6. The following correlation proposed by Vliet and Liu (1969), developed for turbulent flow along a vertical uniformly heated plate, was used for comparison with the CFD results:

$$Nu(x) = 0.568[Gr(x)' Pr]^{0.22} \qquad (10)$$

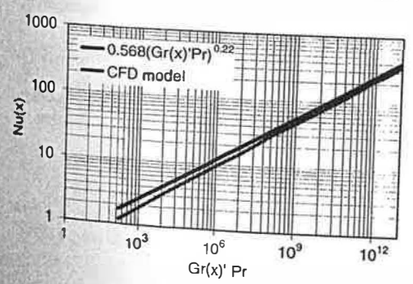

Fig. 6 – Nussel Number

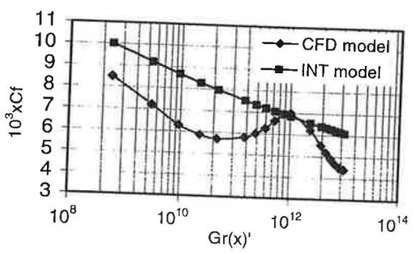

Fig. 7 – Shear stress coefficient

where Pr is the Prandtl number (0.71 for the air) and $Gr(x)'$ is the Grashof number defined as $Gr(x)' = g\beta\rho^2 q_w x^4/(T_{s,0} k \mu^2)$, k being the thermal conductivity of the fluid (air) and $\beta = 1/T_{s,0}$ is the coefficient of thermal expansion. The Nusselt number in the CFD model was obtained from the mean value for the two walls, i.e. $Nu(x) = 1/2\left(Nu(x)^+ + Nu(x)^-\right)$, with $Nu(x)^{\pm} = q_w^{\pm}\, x / \left[\left(T_w^{\pm}(x) - T_{e/2}(x)\right)k\right]$ and $T_{e/2}(x)$ being the temperature at the channel core. As it can be seen, the CFD results agree quite well with those from (10).

In Fig.7 the shear stress coefficient c_f is plotted for the two models. In the INT model c_f was computed from (4), with $a = 0.0592$ and $n = -1/5$, which corresponds to the classic correlation proposed by Schlichting (1979) for characterising the friction coefficient on a flat plate for turbulent flow. In the CFD model c_f was computed for each wall from the corresponding law of the wall, where the well-known dimensionless wall parameters y^+ and u^+ are correlated through a logarithmic law in the inertial sublayer ($y^+ \geq 11.6$). From these parameters the wall shear stress can be deduced, hence c_f, and the mean for the two walls was taken - in a way similar to Nu(x) - to characterise the friction coefficient within the channel.

The c_f value from the CFD model for the range of Gr(x)' show two decreasing zones separated by another where the flow undergoes a sudden increasing, denoting some kind of transition of the flow regime within the system. However, the c_f values computed by this model are systematically lower than those obtained from the INT model. This is certainly one of the reasons for the lower flow rates observed in the latter. If one considers that c_f correlations – like equation (4) - found in literature are normally deduced for forced convection and that are widely used irrespectively of the type of flow (natural or forced convection), the results presented suggest that the pertinence of their use in natural convection is an interesting point to focus on in future studies.

CONCLUSION

In conclusion, the simple model proposed in this work (INT) follows the trends obtained from the more complex CFD model both thermally and dynamically, and produces satisfactory results for general engineering requirements. It would appear that improved results could be obtained from the INT model if skin friction coefficients specific to natural convection flows were used.

REFERENCES

Awbi, H.B. (1996). VORTEX-2, A Computer code for Air Flow, Heat Transfer and Concentration in Enclosures, version 2.1, U.K.

Borgers, T.R. and H. Akbari (1984). Free Convective Turbulent Flow Within the Trombe Wall Channel. *Solar Energy*, **33- 3/4**, 253-264.

Moret Rodrigues, A., A. Canha da Piedade, S. Domingos and S. Valente Pereira (1996). Performance of solar-air collectors for classroom ventilation : Mathematical models versus experimental results. In: Proceedings of the 4th European Conference *Solar Energy in Architecture and Urban Planning*, pp. 472-475, Berlin.

Schlichting, H. (1979). *Boundary Layer Theory*. McGraw-Hill, 7th Ed., New York.

Vliet, G. C. and C. K. Liu (1969). An Experimental Study of Natural Convection Boundary Layers. *J. Heat Transfer*, **91C**, 517-531.